Experimental and modelling evidence of short-term effect of raindrop impact on hydraulic conductivity and overland flow intensity

Claude Mügler, Olivier Ribolzi, Jean-Louis Janeau, Emma Rochelle-Newall, Keooudone Latsachack, Chanthamousone Thammahacksa, Marion Viguier, Emilie Jardé, Thierry Henri-Des-Tureaux, Oloth Sengtaheuanghoung, et al.

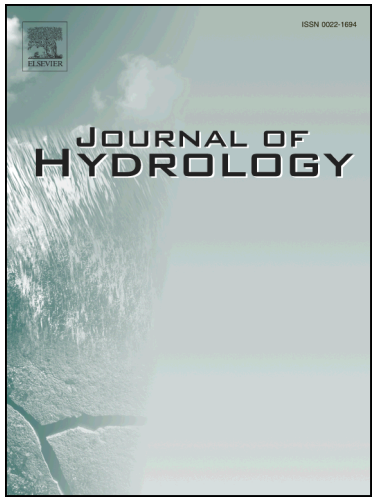

Research papers

Experimental and modelling evidence of short-term effect of raindrop impact on hydraulic conductivity and overland flow intensity

Claude Mügler, Olivier Ribolzi, Jean-Louis Janeau, Emma Rochelle-Newall, Keoudone Latsachack, Chanthamousone Thammahacksa, Marion Viguier, Emilie Jardé, Thierry Henri-Des-Tureaux, Oloth Sengtaheuanghoung, Christian Valentin

PII: S0022-1694(19)30022-8
DOI: https://doi.org/10.1016/j.jhydrol.2018.12.046
Reference: HYDROL 23374

To appear in: *Journal of Hydrology*

Received Date: 20 June 2018
Revised Date: 7 December 2018
Accepted Date: 12 December 2018

Please cite this article as: Mügler, C., Ribolzi, O., Janeau, J-L., Rochelle-Newall, E., Latsachack, K., Thammahacksa, C., Viguier, M., Jardé, E., Henri-Des-Tureaux, T., Sengtaheuanghoung, O., Valentin, C., Experimental and modelling evidence of short-term effect of raindrop impact on hydraulic conductivity and overland flow intensity, *Journal of Hydrology* (2019), doi: https://doi.org/10.1016/j.jhydrol.2018.12.046

Experimental and modelling evidence of short-term effect of raindrop impact on hydraulic conductivity and overland flow intensity

Claude Mügler[a,*], Olivier Ribolzi[b], Jean-Louis Janeau[c], Emma Rochelle-Newall[c], Keooudone Latsachack[d], Chanthamousone Thammahacksa[d], Marion Viguier[d], Emilie Jardé[e], Thierry Henri-Des-Tureaux[d], Oloth Sengtaheuanghoung[f], Christian Valentin[c]

[a] Laboratoire des Sciences du Climat et de l'Environnement, UMR 8212 CEA-CNRS-UVSQ, Orme des Merisiers, 91191 Gif-sur-Yvette Cedex, France

[b] Géosciences Environnement Toulouse, UMR 5563 CNRS-UPS-IRD, 14 avenue Edouard Belin, 31400 Toulouse, France

[c] iEES-Paris, Institut d'Ecologie et des Sciences de l'Environnement de Paris, (IRD, Sorbonne Université, CNRS, INRA, UPEC, Université Paris Diderot), CC237, 4 place Jussieu, 75005 Paris, France

[d] IRD-iEES-Paris, Institut d'Ecologie et des Sciences de l'Environnement de Paris, Department of Agricultural Land Management (DALaM), P.O. Box 4199, Ban Nongviengkham, Xaythany District, Vientiane, Lao PDR

[e] Univ Rennes, CNRS, Géosciences Rennes, UMR 6118, 35000 Rennes, France

[f] Agriculture Land-Use Planning Center (ALUPC), Ministry of Agriculture and Forestry, Vientiane, Lao PDR

Corresponding author: Claude Mügler, claude.mugler@cea.fr

Summary: Tropical montane areas of Southeast Asia are exposed to high-intensity rainfall during the monsoon period. This is particularly problematic in areas where soils on steep slopes are cultivated as it can lead to heavy runoff, high soil erosion, and water pollution. The objective of this paper is to analyse the effect of the impact of raindrops on the dynamics of runoff on such steep fields. Experiments under simulated rainfall were performed at the plot scale (1 m^2) to quantify water export from the surface of upland agricultural soils during overland flow events. Four 1 m^2 plots were divided in duplicated treatment groups: (a) control with no amendments, and (b) amended with pig manure. Each plot was divided into two 0.5 m^2 rectangular subplots. One subplot was designated as a rain splash treatment; the other sub-plot was covered with a 2 mm grid size wire screen that was located 12 cm above the soil surface. The purpose of the screen was to break the raindrops into fine droplets and to reduce fall height in order to drastically reduce their kinetic energy. Runoff was measured for each sub-plot. The results show that raindrop impact drastically enhances runoff generation on both bare soils and on manure amended soils. When the impact of raindrops was limited by screening, runoff was higher on amended soils than on bare soils.

The temporal evolution of runoff was correctly modelled using a soil hydraulic conductivity that exponentially decreases over time of exposure to rainfall. Both experimental and modelling results showed that droplet energy induces a rapid evolution of the hydraulic properties of the soil surface due to crusting, resulting in a reduction of hydraulic conductivity and a concomitant increase in runoff rate.

Keywords: Runoff modelling; Raindrop impact; Hydraulic conductivity; Soil crusting; Tropical agro-ecosystems; Lao PDR

1 Introduction

High intensity rainfall, such as occurs during tropical monsoons, induces reduced infiltration in bare soils (Valentin, 1991; Silburn and Connoly, 1995; Assouline and Mualem, 1997; Fohrer et al., 1999). This is due to the fact that when a raindrop impacts a bare soil surface, its kinetic energy is transferred to the soil surface where it can induce soil compaction, aggregate destruction, particle detachment and splashing. The raindrop impact threshold (related to a critical kinetic energy), specific for each soil type, needs to be overcome in order to initiate and support soil detachment (Armenise et al., 2018). The formation of structural crusts at the surface of bare soils subject to the impact of raindrops depends on the soil properties, rainfall characteristics, flow conditions (e.g. Valentin and Bresson, 1992; Assouline, 2004), and also on the slope gradient (Ribolzi et al., 2011). If fine particles resulting from detachment and/or aggregate destruction are redistributed at the surface or transported by infiltrated water into the upper layer of the soil, they can clog the porosity. The formation of this surface seal drastically reduces infiltration during rainfall (Assouline and Mualem, 1997). Surface sealing depends on soil properties, presence and characteristics of aggregate and organic matter at the soil surface, land-use practices (Rawls et al., 1990, and references therein), but also on rainfall intensity, and drop characteristics (Assouline and Mualem, 1997; Lacombe et al., 2018). All of which can have important implications for soil erosion and overland flow dynamics and water quality particularly in areas with steep slopes and where land use change has led to large areas of bare soil (Valentin et al., 2008; Vigiak et al., 2008; Ziegler et al., 2009; Ribolzi et al., 2017).

In order to quantify the raindrop impact on runoff, Ziegler et al. (2000) performed rainfall simulation experiments on plots covered or not with a wire screen. These authors showed that, even on highly compacted road surfaces, rain splash enhanced runoff. They attributed this enhancement to the sealing of the surface by redistribution of already-detached materials. An et al. (2012), using a similar method, also observed that runoff rates were reduced during rainfall when the raindrop impact was reduced by a net. Only gentle slope gradients (<18%) were investigated. Both Ziegler et al. (2000) and An et al. (2012) focused their study on erosion. None of them modelled runoff enhancement by splash effect.

Experimental studies have yielded contradictory results about the effect of presence of manure on the soil surface on infiltration. On one hand, reductions of infiltration have been observed on manured soils. This was proposed to be a consequence of the plugging of pores by manure particles at the soil surface (Bottom et al., 1986). On the other hand, studies showed infiltration increases after application of manure (Mostaghimi et al., 1989; Gilley et al., 2000), with an increasing effect with the manure application rates. This behaviour was explained by the protecting effect of the manure applied at the soil surface, which reduced the sealing raindrop impact (Roberts and Clanton, 2000). However, given that the texture and water content of manure varies as a function of the source and probably the diet of the species in question, the differences observed may also be due to differences in manure source. Moreover, variability in soil type and texture probably also play an important role.

Physically-based models that numerically solve mass and momentum conservation equations have been widely developed and used in hydrology. An overview of these models and their applications have recently been discussed by Paniconi and Putti (2015) and by Fatichi et al. (2016). These models are particularly useful for simulating the partitioning between infiltration

and runoff. A first attempt to couple overland flow and soil infiltration models was made by Smith and Woolhiser (1971). This approach was successfully tested on laboratory and field experiments. The resulting event-oriented, physically-based runoff and erosion model KINEROS is still used today (Woolhiser et al., 1990; Ziegler et al., 2000, Gal et al., 2017). Because they allow to test more or less sophisticated hypothesis on the runoff generation, physically-based models are interesting tools to interpret experiments. For example, the incorporation of time-dependent hydraulic conductivity functions allows simulation of the evolution of a physical seal layer on the soil surface (Silburn and Conolly, 1995; Assouline, 2004). In another study, the Cast3M numerical code was used to test various roughness models to simulate overland flow experiments at plot scale (Mügler et al., 2011).

The purpose of this paper is to answer by both experimental and modelling approaches to the following questions: How much does the raindrop impact modify runoff on steep slope bare fields? Does manure protect or, on the contrary, enhance the degradation of the surface soils during rainfall events? Is this degradation amplified by successive rainfall events?

In this paper, the materials and methods section presents the experiments and the modelling approach. Measured and modelled runoff rate are compared in the results section. This comparison is followed by a general discussion of the relative influence of raindrop impact, manure presence, and successive rainfalls on runoff rates.

2 Materials and Methods

2.1 Experiments

2.1.1 Study area

The rain simulation experiments were carried out in the Houay Pano catchment (67 ha), located at 102°09'50''E, 19°51'00''N, about ten kilometres from Luang Prabang, North Laos. The elevation ranges from 400 m to 750 m above mean sea level. The mean slope gradient of the catchment is 52% (Ribolzi et al., 2011). The climate is tropical sub-humid with an average annual temperature of 25.3°C (Ribolzi et al., 2011). Average annual precipitation is approximately 1260 mm, and is characterized by high rain intensities of up to 280 mm h^{-1} (Valentin et al., 2008). Alfisols, Ultisols, and Entisols occur over about 50%, 30%, and 20% of the catchment area, respectively (Ribolzi et al., 2011). The experimental plots described in the following section are located on Alfisols. Agricultural practice and land use are typical of North Laos with a slash and burn system of production (Rouw et al., 2014). Over the last 15 years, land use has changed from crops (Job's tears, maize, upland rice) and fallow toward teak plantations (Huon et al., 2013; Ribolzi et al., 2017).

2.1.2 Experimental design

Experiments were performed on four $1m^2$ plots installed on a steep slope (47%±2) of the upper part of the catchment (Fig. 1). The site was covered with fallow from 2005 to 2010 and upland rice during 2011. However, this was harvested and the residues burned several months prior to the experiment. Soil texture was measured using the pipette method of Olmstead et al. (1930). Three replicate measurements were conducted per treatment. However, given the proximity of the plots to each other and their location on the hillslope along the same topographic level, the measurements can almost be considered as being 12 replicates of the same soil. The soil characteristics (slope, texture and porosity) are given in Table 1. Soils exhibited a clay loam texture.

(Table 1 here)

Each plot was divided into two sub-plots (1 m downslope × 0.5 m perpendicular to the slope) in order to investigate the effect of the raindrop impact on runoff and erosion (Fig. 1b). This system, inspired by the experiments performed by Ziegler et al. (2000), consists of covering one half of the 1 m^2 plots with a mosquito net so that the raindrops break into fine droplets. The rainfall kinetic energy is therefore drastically reduced before its impact with the ground. The sub-plot without the mosquito net allows the characterisation of the effect of raindrop impact. The four plots were divided into duplicated treatment groups, denoted A and B: controls with no amendments (Ref A and Ref B) or amended with pig manure (Pig A and Pig B). Plots Pig A and Pig B were only partially covered by disconnected small patches of pig manure. Figure 1c illustrates the distribution of the manure on the soil surface of these plots.

(Figure 1 here)

The soil surface features were characterized both before and after the series of rainfall simulations, using the field method proposed by Valentin and Casenave (1992) and extensively used since then (e.g. Podwojewski et al. 2008; Patin et al. 2012; Lacombe et al., 2018). This method, recently described by Patin et al. (2018) is based on an accurate visual assessment of various components of surface features. This requires to use charts or photo-standards to enable each descriptor to calibrate his visual estimate. Students or farmers can assess the same percentages than a well-trained expert, after a training of only few minutes. In this study, field visual assessment was carried out by a well-trained expert. When compared with the data from image analysis, this type of field visual assessment was found be very accurate, and more rapid

and informative than image digitizing method where some confusions can be made (Malam Issa et al., 2011). The main parameters included percentages of surface covered with vegetation, plant litter (crop residues, leaves, seeds), charcoal, free aggregates, free gravel (i.e. not embedded in a crust). Three types of physical crusts were readily distinguished in the field by their morphology: (i) structural crusts where the original aggregate-induced roughness could still be recognized, (ii) erosion crust where this roughness had disappeared, (iii) gravel crusts that embedded coarse elements. Micromorphological examinations of the structural crusts developed in this site showed that they result from the packing of highly stable micro-aggregates and are referred to as packing crusts (Ribolzi et al., 2011). When compacted by raindrops and smoothed by overland flow, this structural crust gradually transforms into an erosion crust characterized by a thin and very compacted smooth plasmic layer (Valentin and Bresson, 1992). When they include gravels, structural or erosion crusts become a gravel crust (Valentin and Casenave, 1992). Due to the low percentages of erosion and gravel crusts in this study, we combined the three types of crusts in one general category 'total crusts' to focus on the changes between free aggregates and free gravel into crusts. The field criterion between these categories is that collecting free aggregates or gravel from the surface does not disturb the soil surface contrarily to what is observed when collecting an aggregate from a structural crust or a gravel from a gravel crust.

2.1.3 Rainfall simulation

Three successive rainfall simulations were conducted during the dry season using a portable rainfall simulator (Fig. 1a) (Janeau et al., 2014). The rain simulator was calibrated 5 times before each simulation and 5 times after each simulation during 2.5 minutes each time to check the stability of the intensity. The simulator was calibrated so as to produce a raindrop size distribution versus rainfall intensity similar to tropical rainfall (Asseline and Valentin, 1978).

Rainfall intensity was held constant at ~90 mm h^{-1} during 60 min. This intensity value was chosen because it corresponds to the median intensity that has been observed over a 10-year period and for which the kinetic energy permits the detachment of soil particles (Podwojewski et al., 2008). The plots were covered with a plastic cover between simulations to prevent the possible modification of the soil surface characteristics and moisture content from natural precipitation.

The first simulated rainfall, denoted R1, was designed to homogenize the hydrodynamic surface conditions and it was carried out without amendment. The second simulated rainfall, denoted R2, was conducted four days after R1, and was carried out following the application of pig manure to the Pig plots two hours before the rainfall simulation (Table 2). The control plots Ref A and Ref B received no amendment. A third simulated rainfall, denoted R3, was carried out 24 h after R2.

(Table 2 here)

A total of twenty-four experiments were performed on the sub-plots: two applications of rainfall (with or without a mosquito net) × two applications of manure (with or without pig manure) × three successive rainfalls × two replicates.

Overland flow from the PVC exit tube of each 0.5 m^2 sub-plot was collected in a large and clean bucket during each rainfall simulation. Overland flow from each sub-plot was measured during 30 s of every minute using a graduated cylinder in order to calculate overland flow volume. This water was then added to the collecting bucket. The time step of 30 seconds was chosen so that sufficient water could be collected over a short enough time period that the rate of change of runoff flow could be determined. The overland flow coefficient, that is equal to the ratio between

the total overland flow and the total rainfall, was determined for each 0.5 m^2 plot during rainfall simulation.

Statistical significance of the effect of manure addition on surface runoff was determined with the Mann-Whitney test and the non-parametric Wilcoxon test was used to determine the significance of the raindrop impact. For both tests significance was set at $p<0.05$.

2.2 Models

2.2.1 General equations

Numerical simulations of overland flow experiments were performed with a physically-based model that simultaneously solves surface and subsurface flows within a Darcy multidomain approach (Weill et al., 2009). In this approach, the Darcy equation, the Richards equation and the diffusive equation that model the flow in the saturated zone, unsaturated zone, and in the runoff layer, respectively, are written in the same way in the whole domain as follows:

$$C(H)\frac{\partial H}{\partial t} - \vec{\nabla}.\left(K(H)\vec{\nabla}H\right) = q, \quad (1)$$

with $H = h + z$, where h and z are the pressure head [L] and the soil elevation [L], respectively. In this single Richards diffusion type equation that describes both surface and subsurface flows, the parameters $C(H)$ [L^{-1}], and $K(H)$ [LT^{-1}] are domain-dependent and are defined both in the runoff layer and in the subsurface domain. In the saturated zone, $C(H)$ and $K(H)$ are equal to the specific volumetric storage, S_s, and to the saturated hydraulic conductivity of the medium, K_s, respectively. In the unsaturated zone, they are equal to the soil capillary capacity, $C_c(h)$, and to the product $K_s \times k_r(h)$ of the saturated hydraulic conductivity with the relative permeability, respectively. The relative permeability is described by the van Genuchten function (van Genuchten, 1980). In the surface domain, the generalized Eq. (1) is equivalent to the diffusive-

wave approximation of the Saint Venant equation associated with the Manning-Strickler flow formula. In this case, h is equal to the water depth in the runoff layer, $C(H)$ is equal to 0 for h<0, and equal to 1 for h≥0, and $K(H)$ is equal to $h^{5/3}/n\sqrt{S}$, where n is the Manning coefficient that characterizes the soil rugosity, and S is the surface slope. We can notice here that in general the kinematic-wave approximation is applied for modelling overland flow on steep slopes instead of the diffusive-wave approximation (Singh, 2002, and references therein). However, under certain conditions such as steady-state cases of channel flow with upstream boundary conditions of zero discharge and finite length of the channel, which are nearly the conditions of the plot experiments, Singh and Aravamuthan (1995) showed that the diffusive-wave approximation was in excellent agreement with the dynamic-wave approximation, whatever the values of the kinematic-wave number and Froude number.

In the generalized Richards Eq. (1), q is a global source/sink term. In the followings, q will be equal to zero in the whole domain except in the runoff layer where it will be equal to the rainfall.

2.2.2 Numerical methods

The model was numerically solved in the framework of the Cast3M simulation platform that has been developed since the eighties at the CEA in France (see the website www-cast3m.cea.fr for more information).

The Darcy multidomain approach and its numerical resolution have already been tested and validated on numerous academic and realistic test cases (Weill et al., 2009, Mügler et al., 2011; Kollet et al., 2017).

Calculations were performed on a 2D vertical domain with an inclined length and a vertical depth equal to 1 m and 5 m, respectively. The 2D mesh was made of 2x2016 cells. The resolution along the slope was equal to 0.5 m. The vertical resolution was very fine at the top of

the subsurface domain (5×10^{-5} m) and coarsened towards the bottom (5×10^{-2} m). Temporal resolution was adaptive, with a maximum value equal to 1 s. No flow boundary conditions were applied at the vertical and bottom sides of the subsurface domain. At the outlet of the runoff layer, a zero water depth gradient boundary condition was applied (Weill et al., 2007). The rainfall was imposed as a source term in the runoff layer. The initial depth of the water table was equal to 2.5 m that is the observed water table depth at the end of the dry season (Ribolzi et al., 2018).

The spatial scheme was solved with a Finite Volume method (Bernard-Michel et al., 2004). We used a direct solver. The time discretization was implicit and the nonlinear terms were solved with an iterative Picard algorithm. In this formulation, the nonlinear parameters were calculated from an underrelaxated water pressure.

2.2.3 Model parametrization

Parameters involved in the generalized Richards Eq. (1) are the Manning coefficient, *n*, the van Genuchten parameters and the residual water content, n_{VG}, α_{VG}, and θ_{res}, the specific volumetric storage, S_s, and the saturated hydraulic conductivity of the medium, K_s. In a first step, we performed a sensitive analysis and model calibration with the KINEROS code (Woolhiser et al., 1990), and the HydroPSO R package (Zambrano-Bigiarini and Rojas, 2013). For the experiments without the mosquito net, results showed that K_s was the more sensitive parameter. The van Genuchten parameters and Manning coefficient influenced results only during the first minutes of experiments at the beginning of runoff. Indeed, at the 1-m^2 plot scale, some parameters such as the Manning coefficient do not have much influence on overland flow. However, calibration of parameters with KINEROS and HydroPSO R failed for the simulations for the experiments with a mosquito net. Indeed, experimental results clearly showed that permeability was not

constant in time. Furthermore, the problem with so many parameters was an ill-posed problem and a calibration performed in a blind manner gave various sets of "optimized" parameters that were very different between similar experiments. As a consequence, we dropped KINEROS and chose to use the Cast3M code to focus the modelling on the decrease of K_s with time. We also tried to minimize the number of parameters to be estimated by using as much as possible values taken from the literature. The values for the Manning's roughness coefficient for overland flow on a bare clay-loam soil that are recommended by Woolhiser (1975) range between 0.012 and 0.033 s $m^{-1/3}$. We chose n=0.015 s $m^{-1/3}$ (Table 3). As mentioned in Table 1, the soil at the experimental site was mainly clayey. Hence, the van Genuchten parameters and the residual water content were chosen to equal the mean values recommended for Clay (Meyer et al., 1997): n_{VG}=1.13, α_{VG}=0.62, and θ_{res}=0.07. Numerical results were not sensitive to the value of the specific storage. It was chosen equal to 10^{-5} m^{-1}.

The hydraulic conductivity is defined as the ratio of the fluid velocity to the hydraulic gradient. It characterizes the permeability of porous media. In the present paper, we investigated the role of the saturated hydraulic conductivity K_s to drive the partitioning of water between runoff and infiltration. The parameter K_s was assumed constant in space at the 1-m^2 plot scale. However, it was assumed to vary with time during the rainfall event. The purpose of this time variation was to model the changes of the soil properties due to the evolution of the soil structure related to the apparition of crusts that reduce the infiltrability. The modelling of the decrease of K_s with time due to seal formation is often modeled with the following exponential function:

$$K_s(t) = K_\infty + (K_0 - K_\infty)e^{-\propto t}, \quad (2)$$

where K_0 and K_∞ are the initial and final hydraulic conductivities [LT^{-1}], respectively (Silburn and Conolly, 1995; Assouline, 2004, and references therein; Ribolzi et al., 2011). The coefficient

$\propto$ quantifies the decay rate of $K_s(t)$. The higher the value of $\propto$, the more strongly the decrease of K_s with time. As we had no information about the depth of the sealing layer during the rainfall experiments, we assumed that K_s did not vary with depth in the soil. The parameter K_s can be considered as an effective parameter for modelling several processes that modify the soil infiltrability during rainfall.

Finally, the parameters K_0, K_∞, and $\propto$ that characterize the decrease of K_s with time according to the time evolution given by Eq. (2) were the only parameters to be estimated (Table 3).

(Table 3 here)

3 Results and discussion

3.1 Surface runoff experiments

The overland flow coefficient, that is equal to the ratio between the total overland flow and the total rainfall, was determined for each 0.5 m^2 plot during the three successive rainfall simulations. Experimental results obtained for the four different plots, Ref A, Ref B, Pig A, and Pig B, and for the three successive simulated rainfalls, R1, R2, and R3, are displayed in Fig. 2.

(Figure 2 here)

On each figure, empty and filled symbols correspond to the sub-plots without and with a mosquito net, respectively. The thick solid lines correspond to the model outputs (see Section 3.2). The comparison of overland flow coefficients with or without a mosquito net clearly shows

the large effect of raindrop impact on runoff (Fig. 2). The values of the total runoff water measured at the outlet of the 0.5 m^2 plots for the three successive simulated rainfalls are plotted in Fig. 3. Here again, the comparison of overland flow with or without a mosquito net using the non-parametric Wilcoxon analysis clearly shows significantly higher values without a mosquito (p-value < 0.001). Hence, the data clearly show that raindrop impact enhances runoff generation regardless of the treatment applied to the sub-plot and the rainfall event.

(Figure 3 here)

Table 4 gives the main surface features of the various sub-plots both before and after the series of rainfall experiments.

(Table 4 here)

Before the first simulated rainfall, 56% to 72% of the surface of the sub-plots was covered with free aggregates. A large part of the remaining surface (19% to 39%) was covered by crusts. After the third rainfall, almost of all the free aggregates disappeared at the surface of the sub-plot submitted to raindrop impact, and the soil surface was mainly covered by crusts (81% to 91%). In contrast, 37% to 47% of the surface of sub-plots without raindrop impact was still covered by free aggregates after the three successive rainfalls, and the crusts covered 41% to 54%.

3.2 Surface runoff modelling

3.2.1 Simulations

Figure 2 gives the evolution over time of both the measured and modelled overland flow coefficients for the eight sub-plots and for the three rainfalls. Empty and filled symbols correspond to the sub-plots without and with the mosquito net, respectively. The characteristics of the time evolutions $K_s(t)$ used for modelling the runoff are given in Table 5.

(Table 5 here)

Overland flow in each sub-plot without a mosquito net was correctly modelled with a fast decreasing $K_s(t)$, with about the same $\propto$ value ($\propto = 4.2\ h^{-1}$), except for the sub-plot Ref A during rainfall R1 for which a lower value was obtained ($\propto = 1.8\ h^{-1}$). In this particular case, the value is explained by a slower increase of the runoff coefficient during the early stages of the experiment (Fig. 2) due to an artifact related to the temporary obstruction of the sub-plot outlets with coarse soil particles. Noticeably, a decrease of K_0 and K_∞ values was observed from one rainfall to the next for sub-plots without a mosquito net. In contrast, overland flow in each sub-plot with a mosquito net was correctly modelled with a slowly decreasing $K_s(t)$, with a nearly ten times smaller value for $\propto$ ($\propto = 0.48\ h^{-1}$). Here again, the values of K_0 and K_∞ decreased from one rainfall to the next. Evolutions of overland flow in the four sub-plots with a mosquito net during the first rainfall R1, before spreading of manure, are very similar. They are all correctly modelled with the same $K_s(t)$. This result illustrates the reproducibility of the experiments.

3.3 Discussion

The twenty-four runoff experiments performed on sub-plots with or without a mosquito net, and with or without pig manure, showed that raindrop impact drastically enhanced runoff generation on both bare soils and on manured amended soils. The temporal evolution of runoff was correctly modelled using a soil hydraulic conductivity that exponentially decreases over time of exposure to rainfall. Both experimental and modelling results can help to distinguish the phenomena that increase runoff.

3.3.1 Effect of raindrop impact

In the sub-plots where the raindrop impact was reduced (with mosquito net), the reproducibility of the experiments was higher (coefficient of variation = 22%) compared to sub-plots exposed to raindrop impact (coefficient of variation = 50%). As shown in Fig. 2, the evolution over time of the overland flow coefficient for the four sub-plots under the first simulated rainfall are very similar. They were all correctly modelled using the same very slowly decreasing hydraulic conductivity (Table 5).

The differences in infiltration rate between unprotected and protected sub-plots could be ascribed to the differences in crusting rates. Prior to the first simulated rainfall, there was no significant difference among the two series of subplots with a mean crusts coverage of 29% ± 4% for the unprotected subplots and 26% ± 9% for the protected subplots. After the three simulated rainfalls, differences were significant with 86% ± 5% and 49% ± 6%, respectively. With a mean increase in crust coverage for the unprotected sub-plots of 57% ± 5% and a mean rate for protected sub-plots of only 23% ± 12%, the role of the mosquito net in protecting soil from crust development was clearly shown. After rainfalls, very few erosion crusts were observed on the plots. In contrast, structural crusts covered ~ 77% to 89% of the sub-plot surfaces without a

mosquito net, and 41% to 54% of the sub-plot surfaces with a mosquito net. The high coverage of the soil with structural crusts is due to the high slope gradient of the plots. Indeed, Ribolzi et al. (2011) showed that erosion crusts preferentially form under gentle slopes while structural crusts mainly develop under steep slopes. Furthermore, the raindrop impact seems to boost the formation of structural crusts.

The formation of a surprisingly high proportion of crusts and the reduction of infiltration rate on all the sub-plots suggest that the mosquito net did not remove kinetic energy completely. Data have been established under this type of rainfall simulator (Asseline and Valentin, 1978) for a rainfall intensity of 90 mm h^{-1}, with a mean drop diameter of 1.34 mm and a falling height of 3.6 m. It gave a mean falling velocity and a kinetic energy equal to 8.4 m s^{-1} and 22.5 J mm^{-1} m^{-2}, respectively. In a crude estimation based on the drop size distribution measured under 90 mm h^{-1} with the rainfall simulator (Asseline and Valentin, 1978), we can consider that half of the droplets with a diameter smaller than 2 mm could pass through the net unhindered. They represent a kinetic energy of 3.8 J mm^{-1} m^{-2}. The other half hit the mosquito net and fall from a 0.12 m height with a reduced velocity and kinetic energy equal to 3.5 m s^{-1} and 1.7 J mm^{-1} m^{-2}, respectively. Similarly, we can consider that all the drops with a diameter larger than 2 mm also hit the mosquito net and fall with a reduced velocity and a kinetic energy equal to 3.5 m s^{-1} and 2.7 J mm^{-1} m^{-2}, respectively. Using these assumptions, the total kinetic energy would be equal to 8.2 J mm^{-1} m^{-2}, which means a reduction of 64%. Other studies have also used a mosquito net to dissipate kinetic energy (e.g. Carmi et al., 2018) but to our knowledge only Yong and Wiersma (1973) attempted to evaluate its impact on the reduction of kinetic energy. Using four layers of standard insect screen set up 5 cm above ground and high-speed photographs to evaluate the velocity of drops, they estimated that the falling velocity and kinetic energy were reduced by 51-66% and 76-89%, respectively. Our approximation seems consistent with these data because we

used only one layer of mosquito net that was placed further from the ground (12 cm instead of 5 cm). The cumulative kinetic energy of the three high-intensity rainfalls is equal to 2214 J m^{-2}, which is therefore high enough to induce the development of crusts on protected sub-plots. This mean increase in crust coverage for the unprotected sub-plots is about half the mean rate for protected sub-plots, which also seems consistent with a reduction of 64% of the kinetic energy. It is well established that the development of crusts increases with cumulative kinetic energy (e.g. Baumhardt et al., 1990; Armenise et al., 2018).

These results show that runoff is much higher in the sub-plots without a mosquito net (Figs. 2-3), clearly illustrating the well-known impact of raindrops on runoff generation and erosion (Silburn and Connoly, 1995; Assouline and Mualem, 1997; Fohrer et al., 1999; Lacombe et al., 2018). When the impact of raindrops was reduced, total runoff was on average reduced by 70% (Fig. 3). This reduction is much higher than the one hour-averaged reduction of 4% measured by An et al. (2012) on a gentle (9%) slope, with a Mollisol, and with a 100 mm h^{-1} rainfall intensity. However, in these simulated rainfall experiments, the elimination of raindrop impact induced a strong reduction of the runoff rate (1.13% up to 84%) at the beginning of the rainfall (until ~20 min). The authors mentioned that the main factor was rill initiation because they were using 8-m long soil pans under laboratory conditions, conditions that were very different from 1 m-long plots.

The important development of crusts on the Houay Pano soils can be linked to their texture, but also to their content of a relatively high proportion of swelling clays (Valentin 1994; 1997). The reduction of infiltration in swelling soils has been theoretically discussed for some time (Giraldez and Sposito, 1985). However, a quantitative analysis of X-ray Computed Tomography images of soil seal development under simulated rainfall has only recently been performed

(Armenise et al., 2018). This study showed that for a silty clay loam with an initial porosity equal to 0.24, the porosity of the first 5 mm was reduced by a factor of about two, which is a large reduction but this may be due to crust formation rather than to porosity closure due to swelling clay. Aksu et al. (2015) investigated the swelling of clay minerals and its impact on the permeability of unconsolidated porous media. Their experimental results confirmed that permeability decreases with increasing clay content. However, in high porosity samples (more than 36-40%), they showed that the reduction in porosity due to clay swelling was insufficient to cause a meaningful reduction of permeability. In the present experiments, the high soil porosity (~ 58%, cf. Table 1) may explain the weak reduction of infiltration due to swelling effects. Moreover, no cracks were observed prior to the experiments. Where cracks have been observed prior to rainfall simulations, they tended to close very rapidly (Casenave and Valentin, 1989), which cannot explain the gradual reduction of infiltration under the mosquito net. Furthermore, if the closing of cracks were the main process of infiltration reduction, it should be similar in the two series of sub-plots. Instead, a clear difference has been observed, which can be more surely ascribed to the difference in kinetic energy and resulting crusting.

During the first rainfall, experiments performed on the sub-plots protected by a mosquito net differ from those performed without net only by the rainfall characteristics: droplet size and kinetic energy. As already discussed, without raindrop impact, results are reproducible: runoff slowly increases during the rainfall event in the same manner (Fig. 2).

In contrast, with raindrop impact, the results are influenced by the plot characteristics: runoff is higher in Plots A than in Plots B (Fig. 2). According to Rawls et al. (1990), surface sealing depends on soil properties, presence and characteristics of aggregates and organic matter at the soil surface, and to land-use practices. Assouline and Mualem (1997) showed that it also depends

on rainfall characteristics. All the sub-plots had the same soil properties (Table 1), same land-use practices, and were subject to the same rainfall intensity, with identical drop characteristics. However, they did not have exactly the same surface features (Table 4). The variability of infiltrability on bare plots has already been observed in the Houay Pano catchment. Patin et al. (2012) proposed that infiltrability during a natural rainfall event should be considered as a random function in space and time that is described, for each land use, by a log normal probability density function. For bare soils, they obtained a median infiltrability and a geometrical standard deviation equal to 10 mm h^{-1} and 2.9 mm h^{-1}, respectively. The infiltrabilities obtained in our experiments after three rainfall simulations (between 15 and 23 mm h^{-1}, Table 5) are in this range of values, ([10/2.9; 10×2.9]), reflecting the local variations of initial surface properties.

3.3.2 Manure effect

When the raindrop impact is reduced by the mosquito net, the results are also reproducible during the second and third simulated rainfalls, *i.e.* after the amendment with pig manure of two of the sub-plots (Table 5). However, the overland flow coefficient on amended soils increased more rapidly than on bare soils (Fig. 2). Comparison of total runoff on soils with or without manure (Fig. 3) using the non-parametric Mann-Whitney analysis shows significantly higher runoff on manured soil (p-value < 0.05). The decrease of infiltration on manured soils can be explained by the plugging of pores by manure particles at the soil surface (Bottom et al., 1986). In contrast, when the raindrop impact is reduced by the mosquito net, the protecting role of various types of manures that has been observed and described in the literature (Mostaghimi et al., 1989; Gilley et al., 2000; Roberts and Clanton, 2000) becomes much less important. The experimental results also show that when bare soil is protected from raindrop impact, the

presence of pig manure at the surface reduces infiltration by a factor of about two. In the field, plants can play the same role as the mosquito net by protecting the soil from the raindrop effect. Hence, higher runoff may be expected on vegetated fields where pigs are free to roam. This overland flow enhancement can facilitate the transport of bacteria that are present in the manure, and consequently can deteriorate water quality (Ackerman and Taylor, 1995; Choudhary et al., 1996; Ramos et al., 2006).

Results of the experiments with raindrop impact are very different. The evolution over time of the overland flow coefficients depend more on initial soil surface features than on the presence or not of manure. Overland flow coefficients on plots A are always higher than those measured on plots B, even during the first rainfall when there is no manure applied at the soil surface (Fig. 2). Non-parametric Mann-Whitney analysis of total runoff shows no significant difference between bare and manured soils (p-value>0.05). The manure application rates were perhaps too small to have a protecting effect and to reduce the sealing raindrop impact as suggested by Roberts and Clanton (2000). Furthermore, plots A and B were only very partially covered by disconnected small patches of pig manure although Roberts and Clanton added slurry to swine and dairy manure to completely cover the soil surface of their experimental columns.

3.3.3 Modelling of K_s

Runoff experiments were modelled with the Darcy continuum approach described in Section 2.2, with a soil hydraulic conductivity that exponentially decreases over time of exposure to rainfall. The formation of structural crusts observed after three successive rainfalls (Table 4) can explain this decrease. Almost all runoff experiments on sub-plots without a mosquito net were correctly modelled with the same α value ($\propto = 4.2\ h^{-1}$), which corresponds to a strong decrease of infiltrability during the rainfall events. Ribolzi et al. (2011) expressed $\propto$ as the ratio of the

rainfall intensity R and a dimensioning parameter τ. From experiments performed on 30% and 75% slope at the plot scale, they showed that less permeable erosion crusts formed on the 30% slope than the structural crusts that formed on the 75% slope. They obtained τ = 12 mm and 26 mm for the 30% and 75% slope, respectively. In the present study, we obtain τ = 22 mm for a 50% slope. This value further highlights the strong dependence of infiltration rate on slope. In contrast to this value of α, all of runoff experiments with a mosquito net required a much smaller value of α (α=0.48 h^{-1}). Such a value of α results in a very slow and quasi-linear decrease of $K_s(t)$.

The assumption that K_s is constant over soil depth is subject to question as the modified hydraulic conductivity should only be imposed in the sealing layer. Several studies have shown that seal thickness depends on rainfall characteristics (Farres, 1978; Bedaiwy, 2008). The increase of seal thickness with increasing rainfall duration was recently quantified from high-resolution X-ray Computed Tomography images of soil seal development under simulated rainfall (Armenise et al., 2018). For a silty clay loam soil, the seal thickness increased from ~1 mm after 2 min of rainfall to 5.4 mm after 14 min of rainfall. However, as no information is available about the seal or crust thickness on the present plots, we preferred not to add a new unknown parameter. Furthermore, in layered media, the median permeability is controlled by the least permeable layer.

3.3.4 Effect of successive rainfalls

As can be clearly seen in Fig. 2, for each plot, the overland flow coefficient increases during successive rainfalls. For a given plot, this increase is correctly modelled by a decrease of the initial hydraulic conductivity K_0 from one rainfall to the next (Table 5). The experiments were performed in May just before the beginning of the rainfall season. The first simulation provides

an indication of the behaviour of dry, bare soils at the beginning of the monsoon, with an infiltration capacity that progressively decreases over time of exposure to rainfall. Even if there was a four-day gap between the first and second simulated rainfall, the soil did not regain its initial properties. Indeed, the leading cause of infiltration reduction was not the reversible clay swelling but rather the irreversible crusting of the soil surface. As more rain fell, more structural crusts were formed and the soil became less and less permeable.

4 Conclusion

Twenty-four rainfall simulation experiments performed with or without raindrop impact on bare or amended soils led to the following conclusions:

- Raindrop impact drastically enhanced runoff generation on bare soils. When raindrop impact was reduced, runoff was on average reduced by 70%.
- The energy of the raindrops induced a rapid evolution of the hydraulic properties of the soil resulting in a reduction of the hydraulic conductivity and a concomitant increase in runoff intensity.
- A soil hydraulic conductivity that exponentially decreased over time of exposure to rainfall correctly modelled the temporal evolution of runoff.
- Under high intensity rainfall, runoff on soils amended with pig manure was the same as on bare soils. In contrast, when the impact of raindrops was reduced with a 2-mm grid size wire screen, runoff on amended soils was more than twice that of bare soils.
- Soil exposed to successive rainfalls became less and less permeable.

One of the main conclusions of this study is that on steep slopes and under high kinetic energy rainfall conditions, surface runoff is very high and even a low cover, such as a mosquito net, can

significantly reduce it. This result is in agreement with recent studies that showed that when cultivation is abandoned, which is the current tendency in Vietnam, natural regrowth reduces runoff (Lacombe et al., 2016).

The next step of this work will be to characterize the transport of faecal indicator bacteria from these steep slopes under high intensity rainfall. Indeed, increased microbial pathogen dissemination and contamination of stream waters are crucial problems in rural Southeast Asia. For the estimate of the flood and health risk, it is essential that the future simulations better describe surface runoff and erosion at the catchment scale and take into account not only the spatial heterogeneity of the soil hydraulic conductivity but also its temporal evolution.

Acknowledgments

The authors would like to thank the Lao Department of Agriculture Land Management (DALAM) and the Multiscale Tropical Catchments observatory (M-TROPICS; https://mtropics-fr.obs-mip.fr/) for their support. This research was funded by French National Research Agency (TecItEasy project; ANR-13-AGRO-0007), the French Institut de Recherche pour le Développement (IRD) through UMR iEES-Paris and UMR GET and the Pastek program of the GIS-Climat. The authors are thankful to two anonymous reviewers for their suggestions and constructive comments.

References

Ackerman, E.O., Taylor, A.G., 1995. Stream impact due to feedlot runoff, in: Steele, K. (Ed.), Animal Waste and the Landwater Interface. Lewis Publishers, Boca Raton, FL, pp. 119-125.

Aksu, I., Bazilevskaya, E., Karpyn, Z.T., 2015. Swelling of clay minerals in unconsolidated porous media and its impact on permeability. GeoRes. J. 7, 1-13.

An, J., Zheng, F., Lu, J., Li, G., 2012. Investigating the role of raindrop impact on hydrodynamic mechanism of soil erosion under simulated rainfall conditions. Soil Sci. 177(8), 517-526.

Armenise, E., Simmons, R.W., Ahn, S., Garbout, A., Doerr, S.H., Mooney, S.J., Sturrock, C.J., Ritz, K., 2018. Soil seal development under simulated rainfall: Structural, physical and hydrological dynamics. J. Hydrol. 556, 211–219.

Asseline, J., Valentin, C., 1978. Construction et mise au point d'un infiltromètre à aspersion. Cah. ORSTOM, sér. Hydrol., vol. XV, n° 4, 321-349.

Assouline, S., Mualem, Y., 1997. Modeling the dynamics of seal formation and its effect on infiltration as related to soil and rainfall characteristics. Water Resour. Res. 33(7), 1527-1536.

Assouline, S., 2004. Rainfall-induced soil surface sealing: A critical review of observations, conceptual models, and solutions. Vadose Zone J. 3, 570-591.

Baumhardt, R.L., Römkens, M.J.M., Whisler, F.D., Parlange, J.Y., 1990. Modeling infiltration into a sealing soil. Water Resour. Res., 26(10), 2497-2505.

Bedaiwy, M.N.A., 2008. Mechanical and hydraulic resistance relations in crust topped soils. Catena 72 (2), 270–281.

Bernard-Michel, G., Le Potier C., Beccantini A., Gounand S., Chraibi, M., 2004. The Andra Couplex 1 test case: Comparisons between finite-element, mixed hybrid finite element and finite volume element discretizations. Comput. Geosci. 8, 187–201, 2004.

Bottom, J.D., Taraba, J.L., Ross, I.J., 1986. Infiltration rate reduction on dairy manured plots. ASAE Paper No. 86-4057.

Carmi, G., Abudi, I., Berliner, P., 2018. An experimental study to assess the effect of the energy and the electrolyte concentration of rain drops on the infiltration properties of naturally crusted soils. J. Arid Environ. 152, 69-74.

Casenave, A., Valentin, C., 1989. Les états de surface de la zone sahélienne. Influence sur l'infiltration. ORSTOM, Collection "Didactiques". 230 p.

Choudhary, M, Bailey, L.D., Grant, C.A., 1996. Review of the use of swine manure in crop production: effects on yield and composition and on soil and water quality. Waste Manag. & Res. 14, 581-595.

Farres, P., 1978. Role of time and aggregate size in the crusting process. Earth Surf. Proc. 3 (3), 243–254.

Fatichi, S., Vivoni, E.R., Ogden, F.L., Ivanov, V.Y., Mirus, B., Gochis, D., Downer, C.W., Camporese, M., Davison, J.H., Ebel, B., Jones, N., Kim, J., Mascaro, G., Niswonger, R., Restrepo, P., Rigon, R., Shen, C., Sulis, M., Tarboton, D, 2016. An overview of current applications, challenges, and future trends in distributed process-based models in hydrology. J. Hydrol. 537, 45-60.

Fohrer, N., Berkenhagen, J., Hecker, J.-M., Rudolph, A., 1999. Changing soil and surface conditions during rainfall: Single rainstorm/subsequent rainstorms. Catena 37, 355–375.

Gal, L., Grippa, M., Hiernaux, P., Pons, L., Kergoat, L., 2017. The paradoxical evolution of runoff in the pastoral Sahel: analysis of the hydrological changes over the Agoufou watershed (Mali) using the KINEROS-2 model. Hydrol. Earth Syst. Sci. 21, 4591-4613.

Gilley, J.E., Risse, L.M., 2000. Runoff and soil loss as affected by the application of manure. Trans. Am. Soc. Agric. Eng. 43(6), 1583-1588.

Giraldez, J.V., Sposito, G., 1985. Infiltration in swelling soils. Water Resour. Res. 21(1), 33-44.

Huon, S., de Rouw, A., Bonté, P., Robain, H., Valentin, C., Lefèvre, I., Girardina, C., Le Troquer, Y., Podwojewski, P., Sengtaheuanghoung, O., 2013. Long-term soil carbon loss and accumulation in a catchment following the conversion of forest to arable land in northern Laos. Ag. Ecosys. Environ. 169, 43-57.

Janeau, J.L., Gillard, L.C., Grellier, S., Jouquet, P., Le, T.P.Q., Luu, T.N.M., Ngo, Q.A., Orange, D., Pham, D.R., Tran, D.T., Tran, S.H., Trinh, A.D., Valentin, C., Rochelle-Newall, E., 2014. Soil erosion, dissolved organic carbon and nutrient losses under different land use systems in a small catchment in northern Vietnam. Agric. Water Manage. 146, 314-323.

Kollet, S., Sulis, M., Maxwell, R., Paniconi, C., Putti, M., Bertoldi, G., Coon, E.T., Cordano, E., Endrizzi, S., Kikinzon, E., Mouche, E., Mügler, C., Park, Y.-J., Stisen, S., Sudicky, E., 2017. The integrated hydrologic model intercomparison project, IH-MIP2: A second set of benchmark results to diagnose integrated hydrology and feedbacks. Water Resour. Res. 53, 867-890.

Lacombe, G., Ribolzi, O., de Rouw, A., Pierret, A., Latsachak, K., Silvera, N., Pham Dinh, R., Orange, D., Janeau, J.-L., Soulileuth, B., Robain, H., Taccoen, A., Sengphaathith, P., Mouche E., Sengtaheuanghoung, O., Tran Duc, T., Valentin, C., 2016. Contradictory hydrological impacts of afforestation in the humid tropics evidenced by long-term field monitoring and simulation modelling. Hydrol. Earth Syst. Sci. 20, 2691–2704.

Lacombe, G., Valentin, C., Sounyafong, P., de Rouw, A., Soulileuth, B., Silvera, N., Pierret, A., Sengtaheuanghoung, O., Ribolzi, O., 2018. Linking crop structure, throughfall, soil surface conditions, runoff and soil detachment: 10 land uses analyzed in Northern Laos. Sci. Total Environ. 616, 1330-1338.

Malam Issa, O., Valentin, C., Rajot, J.L., Cerdan, O., Desprats, J.-F., Bouchet, T., 2011. Runoff generation fostered by physical and biological crusts in semi-arid sandy soils. Geoderma 167-168, 22-29.

Meyer, P.D., Rockhold, M.L., Gee, G.W., 1997. Uncertainty Analyses of Infiltration and Subsurface Flow and Transport for SDMP Sites. Scientific Report NUREG/CR-6565 PNNL-11705 of the U.S. Nuclear Regulatory Commission Office of Nuclear Regulatory Research Washington, DC 20555-0001.

Mostaghimi, S., Deizman, M.M., Dillaha, T.A., Heatwole, C.D., 1989. Impact of land application of sewage sludge on runoff water quality. Trans. ASAE 32(2): 491-496.

Mügler, C., Planchon, O., Patin, J., Weill, S., Silvera, N., Richard, P., Mouche, E., 2011. Comparison of roughness models to simulate overland flow and tracer transport experiments under simulated rainfall at plot scale, J. Hydrol. 402, 25–40.

Olmstead, L.B., Alexander, Lyle T., Middleton, H.E., 1930. A pipette method of mechanical analysis of soils based on improved dispersion procedure. U.S. Dept. Agric. Tech. Bull. 170, 1-22.

Paniconi, C., Putti, M., 2015. Physically based modeling in catchment hydrology at 50: survey and outlook. Water Resour. Res. 51(9), 7090-7129.

Patin, J., Mouche, E., Ribolzi, O., Chaplot, V., Sengtahevanghoung, O., Latsachak, K.O., Soulileuth, B., Valentin, C., 2012. Analysis of runoff production at the plot scale during a long-term survey of a small agricultural catchment in Lao PDR. J. Hydrol. 426-427, 79-92.

Patin, J., Mouche, E., Ribolzi, O., Sengtahevanghoung, O., Latsachak, K.O., Soulileuth, B., Chaplot, V., Valentin, C., 2018. Effect of land use on interrill erosion in a montane catchment of

Northern Laos: An analysis based on a pluri-annual runoff and soil loss database. J. Hydrol. 563, 480-494.

Podwojewski, P., Orange, D., Jouquet, P., Valentin, C., Nguyen, V., Janeau, J., Tran, D., 2008. Land-use impacts on surface runoff and soil detachment within agricultural sloping lands in Northern Vietnam. Catena 74, 109-118.

Ramos, M.C., Quinton, J.N., Tyrrel, S.F., 2006. Effects of cattle manure on erosion rates and runoff water pollution by faecal coliforms. J. Environ. Manage. 78, 97-101.

Rawls, W.J., Brakensiek, D.L., Simanton, J.R., Kohl, K.D., 1990. Development of a crust factor for a Green Ampt model. Trans. ASAE 33(4), 1224-1228.

Ribolzi, O., Patin, J., Bresson, L.M., Latsachack, K.O., Mouche, E., Sengtaheuanghoung, O., Silvera, N., Thiébaux, J.P., Valentin, C., 2011. Impact of slope gradient on soil surface features and infiltration on steep slopes in northern Laos. Geomorphology 127, 53-63.

Ribolzi, O., Evrard, O., Huon, S., de Rouw, A., Silvera, N., Latsachack, K.O., Soulileuth, B., Lefèvre, I., Pierret A., Lacombe, G., Sengtaheuanghoung, O., Valentin, C., 2017. From shifting cultivation to teak plantation: effect on overland flow and sediment yield in a montane tropical catchment. Sci. Rep. 7(1), 3987.

Ribolzi, O., Lacombe, G., Pierret, A., Robain, H., Sounyafong, P., de Rouw, A., Soulileuth, B., Mouche, E., Huon, S., Silvera, N., Latxachak K.O., Sengtaheuanghoung, O., Valentin, C., 2018. Interacting land use and soil surface dynamics control groundwater outflow in a montane catchment of the lower Mekong basin. Agric. Ecosyst. Environ. 268, 90-102.

Roberts, R.J., Clanton, C.J., 2000. Surface seal hydraulic conductivity as affected by livestock manure application. Trans. ASAE 43(3), 603-613.

Rouw, A.D., Casagrande, M., Phaynaxay, K., Soulileuth, B., Saito, K., 2014. Soil seedbanks in slash-and-burn rice fields of northern Laos. Weed Res. 54(1), 26-37.

Silburn, D.M., Connoly, R.D., 1995. Distributed parameter hydrology model (ANSWERS) applied to a range of catchment scales unsing rainfall simulator data I: Infiltration modelling and parameter measurement. J. Hydrol. 172, 87-104.

Singh, V.P., 2002. Is hydrology kinematic? Hydrol. Process. 16, 667-716.

Singh, V.P., Aravamuthan, V., 1995. Accuracy of kinematic wave and diffusion wave approximations for time-independent flows. Hydrol. Process. 9, 755-782.

Valentin, C., 1991. Surface crusting in two alluvial soils of northern Niger. Geoderma 48, 201-222.

Valentin, C., Bresson, L.M., 1992. Morphology, genesis and classification of soil crusts in loamy and sandy soils. Geoderma 55, 225-245.

Valentin, C., Casenave, A., 1992. Infiltration into sealed soils as influenced by gravel cover. Soil Sci. Soc. Am. J. 56(6), 1667-1673.

Valentin, C., 1994. Surface sealing as affected by various rock fragment covers in West Africa. Catena 23(1-2), 87-97.

Valentin, C., Bresson, L.-M., 1997. Soil crusting, in: Lal, R., Blum, W.E.H., Valentin, C., Stewart, B.A. (Eds.), Methods for Assessment of Soil Degradation. Advances in Soil Science, pp. 89-107.

Valentin, C., Agus, F., Alamban, R., Boosaner, A., Bricquet, J.P., Chaplot, V., de Guzman, T., de Rouw, A., Janeau, J.L., Orange, D., Phachomphonh, K., Phai, Do. Duy, Podwojewski, P., Ribolzi, O., Silvera, N., Subagyono, K., Thiébaux, J., Toan, T., Vadari, T., 2008. Runoff and

sediment losses from 27 upland catchments in Southeast Asia: Impact of rapid land use changes and conservation practices. Agric. Ecosyst. Environ. 128, 225-238.van Genuchten, M.T., 1980. A closed-form equation for predicting the hydraulic conductivity of unsaturated soils. Soil Sci. Soc. Am. J. 44(5), 892–898, doi:10.2136/sssaj1980.03615995004400050002x.

Vigiak, O., Ribolzi, O., Pierret, A., Sengtaheuanghoung, O., Valentin, C., 2008. Trapping efficiencies of cultivated and natural riparian vegetation of northern Laos. J. Environ. Qual. 37, 889-897.

Weill, S., Mouche, E., Patin, J., 2009. A generalized Richards equation for surface/subsurface flow modelling. J. Hydrol. 366, 9-20.

Woolhiser, D.A., 1975. Simulation of unsteady overland flow, in Mahmood, K., Yevjevich, V. (Eds), Unsteady Flow in Open Channels, v.II, Water Resources Publications, Fort Collins, p. 502.

Woolhiser, D.A., Smith, R.E., Goodrich, D.C., 1990. KINEROS, a kinematic runoff and erosion model: Documentation and user manual. U.S. Department of Agriculture, Agricultural Research Service, ARS-77, 130 pp.

Young, R.A., Wiersma, J. L., 1973. The role of rainfall impact in soil detachment and transport. Water Resour. Res. 9(6), 1629-1636.

Zambrano-Bigiarini, M., Rojas, R., 2013. A model-independent particle swarm optimisation software for model calibration. Environ. Modell. Software 43, 5-25.

Ziegler, A.D., Sutherland, R.A., Giambelluca, T.W., 2000. Partitioning total erosion on unpaved roads into splash and hydraulic components: The roles of interstorm surface preparation and dynamic erodibility. Water Resour. Res. 36, 2787-2791.

Ziegler, A.D., Bruun, T.B., Guardiola-Claramonte, M., Giambelluca, T.W., Lawrence, D., Lam, N.T., 2009. Environmental consequences of demise in swidden cultivation in montane mainland southeast Asia: Hydrology and geomorphology. Hum. Ecol. 37, 361–373.

Figure captions:

Figure 1: Experimental design: (a) rain simulator in the background with the covered plots in the foreground; (b) close-up of the split plot with the mosquito net and blue PVC exit tubes; and (c) distribution of manure 'spots' on the soil surface of the 'Pig' plots.

Figure 2: Evolution of the overland flow coefficients. The first horizontal line displays the three successive simulated rainfalls (90 mm h^{-1} during 60 min). Each other horizontal line, composed of three figures, corresponds to the results obtained from these three successive simulated rainfalls, for a given 1 m^2 plot. On each figure, symbols indicate measured data while the solid lines indicate modelled results. Empty and filled symbols correspond to the sub-plots without and with a mosquito net, respectively. Circles and triangles refer to the Ref or Pig experiments, and the red and blue colours refer to the replicates A and B, respectively. Continuous lines correspond to the modelling results obtained with a decreasing $K_s(t)$ given by Eq. (2) and characterized by the values of the three parameters, $\propto$, K_0, and K_∞. These values are compiled in Table 5.

Figure 3: Total runoff (mm m^{-2}) for the four plots, with or without raindrop impact.

- Raindrop impact enhances soil crusting and therefore runoff generation
- When raindrop impact was reduced, runoff was on average reduced by 70%
- When raindrop impact was reduced, runoff on amended soil was higher than on bare soil
- Soil exposed to successive rainfalls progressively becomes impermeable
- Hydraulic conductivity that exponentially decreases over time correctly models runoff

Table 1: Main soil surface (0-5 cm) characteristics of the four 1 m^2 plots.

	Ref A	Pig A	Ref B	Pig B	Mean
Slope (%)	48	50	43	48	47
Clay (%)	51	48	47	52	50
Silt (%)	30	30	30	30	30
Sand (%)	17	20	20	17	18
Porosity θ_{sat} (%)	56	56	60	59	58

Clay<2 μm; Silt 2-50 μm; Sand 50-2000 μm.

Table 2: Chronology of plot preparation and experiments.

Day from start	Work done
0	Initial rainfall R1 in order to homogenize the hydrodynamic surface conditions
4	Pig manure amended on plots Pig A and Pig B No amendment on the control plots Ref A and Ref B Rainfall R2 two hours after amendment
5	Rainfall R3

Table 3: Values of the parameters for the modelling approach.

Parameter	Symbol	Value	Unity
Hydraulic parameters for overland flow			
Manning's roughness	n	0.015	s $m^{-1/3}$
Hydraulic parameters for subsurface flow			
van Genuchten parameter	n_{VG}	1.13	-
van Genuchten parameter	α_{VG}	0.62	-
Residual water content	θ_{res}	0.07	-
Specific storage	S_s	10^{-5}	m^{-1}
Saturated hydraulic conductivity	$K_s(t)$	$K_\infty + (K_0 - K_\infty)e^{-\propto t}$	m s^{-1}

	K_0	to be estimated	m s^{-1}
	K_∞	to be estimated	m s^{-1}
	α	to be estimated	s^{-1}

Table 4: Main surface features of the eight sub-plots. In each cell of the table the two values correspond to the surface features before and after the three successive rainfall simulations. ~~before/after the three successive rainfall simulations.~~

sub-plot (0.5 m^2)	free aggregates (%)	total crusts (%)	free aggregates (%)	total crusts (%)
	with raindrop impact		**without raindrop impact**	
Ref A	66 ~~/~~ 0.5	27 ~~/~~ 90	72 ~~/~~ 37	19 ~~/~~ 52
Ref B	59 ~~/~~ 2	29 ~~/~~ 81	71 ~~/~~ 38	20 ~~/~~ 54
Pig A	58 ~~/~~ 1	35 ~~/~~ 91	56 ~~/~~ 46	39 ~~/~~ 49
Pig B	65 ~~/~~ 2	26 ~~/~~ 82	64 ~~/~~ 47	26 ~~/~~ 41

Table 5: Calibrated values of the parameters for the $K_s(t)$ evolution obtained for the eight sub-plot experiments (Ref A, Ref B, Pig A, and Pig B, with and without raindrop impact), and for the three successive simulated rainfalls (R1, R2, and R3).

sub-plot	Rainfall	α (h^{-1})	K_0 (mm h^{-1})	K_∞ (mm h^{-1})
without a mosquito net				
Ref A	R1	1.8	93	20
	R2	4.2	70	20
	R3	4.2	40	20
Pig A	R1	4.2	80	33

	R2	4.2	55	15
	R3	4.2	30	15
Ref B and Pig B	R1	4.2	80	48
	R2	4.2	90	43
	R3	4.2	55	23
with a mosquito net				
Ref A and Ref B	R1	0.48	93	65
	R2	0.48	88	65
	R3	0.48	80	65
Pig A and Pig B	R1	0.48	93	65
	R2	0.48	78	20
	R3	0.48	67	20

Tropical montane areas of Southeast Asia are exposed to high-intensity rainfall during the monsoon period. This is particularly problematic in areas where soils on steep slopes are cultivated as it can lead to heavy runoff, high soil erosion, and water pollution. The objective of this paper is to analyse the effect of the impact of raindrops on the dynamics of runoff on such steep fields. Experiments under simulated rainfall were performed at the plot scale (1 m^2) to quantify water export from the surface of upland agricultural soils during overland flow events. Four 1 m^2 plots were divided in duplicated treatment groups: (a) control with no amendments, and (b) amended with pig manure. Each plot was divided into two 0.5 m^2 rectangular subplots. One subplot was designated as a rain splash treatment; the other sub-plot was covered with a 2 mm grid size wire screen that was located 12 cm above the soil surface. The purpose of the screen was to break the raindrops into fine droplets and to reduce fall height in order to drastically reduce their kinetic energy. Runoff was measured for each sub-plot. The results show that raindrop impact drastically enhances runoff generation on both bare soils and on manure

amended soils. When the impact of raindrops was limited by screening, runoff was higher on amended soils than on bare soils.

The temporal evolution of runoff was correctly modelled using a soil hydraulic conductivity that exponentially decreases over time of exposure to rainfall. Both experimental and modelling results showed that droplet energy induces a rapid evolution of the hydraulic properties of the soil surface due to crusting, resulting in a reduction of hydraulic conductivity and a concomitant increase in runoff rate.

Declaration of interests

☒ The authors declare that they have no known competing financial interests or personal relationships that could have appeared to influence the work reported in this paper.

☐The authors declare the following financial interests/personal relationships which may be considered as potential competing interests: